

Evidence of a single-wall platinum nanotube

Yoshifumi Oshima,* Hiroaki Koizumi, Keinosuke Mouri, Hiroyuki Hirayama, and Kunio Takayanagi

Department of Materials Science & Engineering, Tokyo Institute of Technology, 4259 Nagatsuta, Midori-ku, Yokohama 226-8502, Japan

Yukihito Kondo

JEOL Ltd., Akishima, Tokyo 196-8558, Japan

(Received 16 August 2001; revised manuscript received 9 November 2001; published 1 March 2002)

A suspended platinum nanowire was observed to have the same helical multishell structure (HMS) that was reported for gold nanowires thinner than 2 nm. The investigation was made in an ultrahigh vacuum high-resolution electron microscope (JEM-2000VF). The platinum nanowire was synthesized by an electron-beam thinning method at elevated temperatures to enhance the Pt atom migration. A platinum multishell nanowire was thinned by migration until it finally snapped. In the meantime, the outer shell was stripped from a 13-6 HMS to partially expose the inner shell. Simulated electron microscope images supported that the exposed inner shell was a single-wall tube having a tunnel at the wire axis.

DOI: 10.1103/PhysRevB.65.121401

PACS number(s): 68.37.Lp, 61.46.+w, 81.07.De

Gold nanowires are attracting much interest because of their magic structure^{1,2} and conductance.³⁻⁵ Gold nanowires of less than 2 nm in thickness were synthesized by an electron-beam technique in an ultrahigh vacuum electron microscope.¹ The suspended gold nanowire, then, had a helical multishell (HMS) structure, like that of carbon nanotubes.⁶ Unlike a hexagonal network for carbon nanotubes, each shell of the HMS is formed by a triangular network which is similar to the (111) atomic sheet of a gold crystal. The [110] atomic rows in each (111) sheet make a helix that coils around the axis of the gold nanowire. The n - n' - n'' HMS nanowire, then, is composed of n , n' , and n'' atomic rows in each shell, and has a relation that the number of atomic rows in the outer and inner shells differ by seven ($n-n'=7$). The finest HMS has a 7-1 shell structure. Also, the thicker ones have 11-4, 12-5, 13-6, and 14-7-1 shell structures.¹ Recently, Tosatti *et al.* investigated the finest 7-1 HMS theoretically in favor of its existence.⁷ Theoretical MD simulations performed by Bilalbegovic⁸⁻¹⁰ suggested shell-like structures for gold nanowires. Although the theory gave support for the gold HMS,⁷ there is a question as to whether the gold HMS is a tubular structure, like carbon nanotubes, or a condensed solid wire.

A shell structure was reported for condensed solid wires formed by alkaline metals (Na, K, and Li).¹¹⁻¹³ The alkaline nanowires showed pronounced conductance peaks near 1, 3, 5, and 6 G_0 in a conductance histogram at 4.2 K, where the quantum unit of conductance is $G_0=2e^2/h$. The conductance measurement was extended to higher temperatures and to much higher conductance values by A. I. Yanson *et al.*,¹¹ revealing much finer peaks. These conductance measurements suggested a shell model for electrons confined in a cylindrical nanowire, similarly to the shell model for alkaline metal clusters.¹³ For example, sodium clusters¹⁴ show abundance spectra at the magic numbers ($N=2, 8, 20, 40, 58$ EEE). These numbers correspond to the number of valence electrons in a spherical potential well. Since clusters of monovalent noble metals (gold, silver, and copper)^{15,16} were also reported to have a shell model, the gold HMS might have a peculiar electronic structure confining electrons, like alkaline metal nanowires.

The conductances of gold nanowires formed at the quantum point contact (QPC) of gold electrodes were measured by several experiments,^{3,4,17-19} where the nanowires were formed by STM geometry, a mechanically controllable breaking (MCB) junction, or a switching regulator. No indication that shows a shell effect has been found in those reports. They, rather, showed a conductance of $G=2G_0$, which is not allowed for a cylindrical wire because of symmetry. The simultaneous observation of both the conductance and the structure of gold QPC's formed by STM geometry showed that a nanowire which has just two atom rows gave $G=2G_0$.⁴ The experiment also showed a gold nanowire having $G=6G_0$, which is predicted by a recent theoretical calculation⁷ as the conductance of the 7-1 HMS. However, the length of the nanowire was much shorter than the pitch (helicity) of the 7-1 HMS (30 nm).¹ In previous experiments using STM and MCB geometries, neither long nanowires nor the tubular HMS structure seem to have been synthesized.

To conclude whether the gold HMS is tubular or a condensed cylinder, we need to observe finer nanowires than the 7-1 HMS. Because the 7-1 HMS has an atomic chain that fills the central tunnel of the outer shell, which is composed of seven atomic rows, it is interesting to study if any single-wall metal tube can exist in nature or by synthesis.

We studied platinum (Pt) nanowires to examine whether 5 or 6 atomic rows can coil to form a nanotube. We used an electron-beam irradiation technique to fabricate a platinum nanowire *in situ* in an ultrahigh vacuum transmission electron microscope (UHV-TEM), similar to that used in Refs. 1-3. The platinum nanowire showed a transmission electron-microscope image like that of a single-wall carbon nanotube. Two dark lines for the sides of the wall were imaged. The observed widths of the tube were 0.40-0.46 nm, suggesting that six platinum atomic rows coiled around the axis.

A thin platinum film was prepared by the Pashley method.²⁰ A thick silver film (500 nm) was deposited on an air-cleaved NaCl surface at 300 °C, followed by the deposition of platinum on a silver substrate at 300 °C in a high-vacuum chamber. After dissolving the silver film in HNO₃ and NaCl crystal in water, a platinum film having a thickness

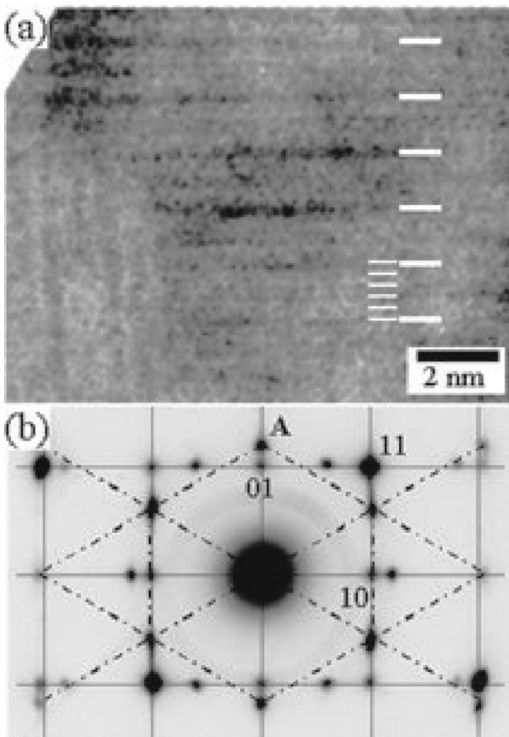


FIG. 1. (a) Transmission electron-microscope image of platinum (001) film after thinning by electron-beam irradiation. The lattice fringes (indicated by thin white lines) have a spacing of $a=0.277$ nm for the platinum (001) lattice, whose intensity is modulated with a period of $5a$, as indicated by the thick white lines. (b) Transmission electron diffraction around the area shown in (a). In addition to the reciprocal spots of the Pt(001) lattice (connected by dotted lines), those from the hexagonal surface layer appear (connected by dotted-dashed lines). The platinum surface has a 5×1 reconstructed structure, since the distance between the spot A and the 01 spot is one fifth of the basic reciprocal lattice. Two domains of the 5×1 structure are formed.

within 3–5 nm was mounted on a carbon microgrid with holes (average hole size, $2 \mu\text{m}$) following the conventional manner. A spectroscopic analysis (EDS) of the platinum film could detect no fluorescent X-ray signal of silver atoms. The platinum film was then heated to 400°C in a UHV-TEM (JEM-2000VF) using a heating specimen holder. The thin platinum film was irradiated by a strong electron-beam ($300 \text{ A}/\text{cm}^2$) for thinning the surface. After several hours of irradiation, high-resolution transmission electron microscope (HR-TEM) images of the platinum (001) film showed fringes with a spacing of $5a$, where a is the basic lattice constant of the ideal platinum (001) surface ($a=0.277$ nm) [Fig. 1(a)]. Such a TEM image and diffraction pattern, such as those in Fig. 1(b), indicate that the surface of the platinum film has a 5×1 reconstructed structure in which the outermost surface layer has reconstructed to a hexagonal lattice. This appearance of the 5×1 surface reconstruction is well known as an indication of a clean platinum (001) surface;^{21,22} the platinum (001) 5×1 reconstructed surface structure only exists when the surface has a small amount of carbon and other contaminations detectable by Auger spectroscopy. Therefore, platinum nanowires that are formed by further thinning are

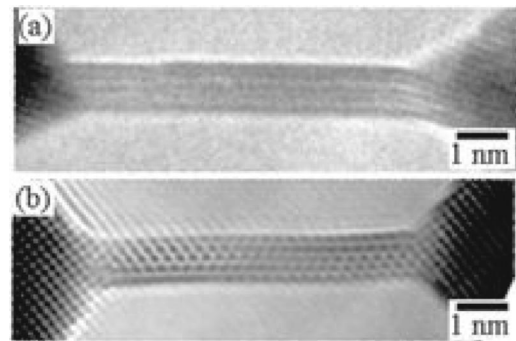


FIG. 2. (a) HR-TEM image of a platinum nanowire. The apparent width of the nanowire is 0.98 nm. Five dark lines in the nanowire slightly wander from the wire axis (seen at a glancing angle from the direction of the wire axis). Simulated TEM images of the platinum 13-6 HMS having $d=0.28$ nm and a diameter of 1.0 nm (not shown), have apparent widths of 0.98–1.00 nm. (b) HR-TEM image of a gold nanowire having the 13-6 multishell structure reported in Ref. 2. The apparent width of the image is around 0.98 nm (the diameter of the model is 1.04 nm, and $d=0.29$ nm).

supposed to be kept free from carbon and other contaminations. During irradiation, holes were created at many places. A platinum wire was formed between two neighboring holes. In this procedure, we needed to heat the platinum film to synthesize long platinum nanowires by enhancing the diffusion.

After more than 10 h of irradiation, the wire had a diameter on the order of one nanometer. We then reduced the beam intensity to $20 \text{ A}/\text{cm}^2$ and recorded any change of the nanowire on a videotape through a television camera (Gatan-622) attached to the UHV-TEM with a speed of 30 frames per second. Figure 2(a) shows a HR-TEM image of the platinum nanowire. The image shows five dark lines, having characteristics that represent HMS;¹ these lines slightly wander from the wire axis. The distance between the outer dark lines modulates slightly because of the helical structure, and the apparent width of the platinum nanowire image is 0.98 nm. Figure 2(b) is a typical image of a gold nanowire having the 13-6 HMS, which shows an image with five atomic rows along the wire axis (Fig. 4 in Ref. 2). The gold 13-6 nanowire has a theoretical diameter of 1.04 nm, and the image has an apparent width of 0.96 nm. TEM images of platinum nanowires had poor resolution, because of mechanical vibration caused by the heating holder. We simulated TEM images by the multislice calculation method,^{23,24} and carefully compared them with the observations. The same imaging conditions as in Ref. 2 (200 kV, $C_s=0.7$ mm, $C_c=1.2$ mm, $\Delta V/V=10^{-5}$, $\alpha=10^{-3}$ rad) were chosen for the simulation. The image degradation due to the vibration was taken into account by convoluting a simulated image intensity with a Gauss function along the wire axis (half width: 0.02 nm) as a blurring function. We chose 11-4, 12-5, 13-6, and 14-7-1 HMS models for the platinum nanowire. We assumed the same pitch (helicity) as that of the gold HMS nanowires,² choosing the atomic distance of the [110] atom row, $d=0.28$ nm ($d=0.29$ nm for gold) for platinum. The simulated image of the platinum 11-4 nanowire showed four wavy dark lines (image of 4 lines). The 12-5 nanowire image

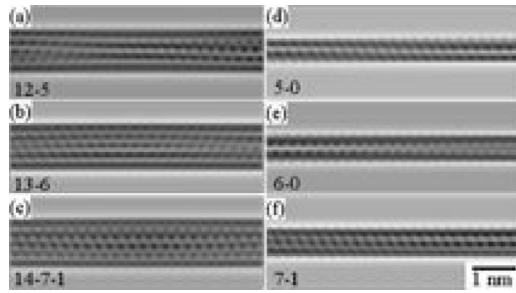


FIG. 3. (a), (b), and (c): Simulated images of platinum 12-5 (period of the helix is 83 nm), 13-6 (139 nm) and 14-7-1 (162 nm) nanowires, respectively. (d), (e), and (f): The simulated images of 5-0 (period of the helix is 83 nm and diameter is 0.41 nm), 6-0 (139 nm and 0.48 nm) and 7-1 (162 nm and 0.55 nm) nanowires, respectively. These images are degenerated by a convolution of the Gauss function along the wire axis (half width, 0.02 nm). Since the pitch of the nanowires were long, we only showed a part of the nanowire (longer than the length L/n , where L is the pitch and n is the number of the atomic row composing the outermost tube).

showed four lines and five lines periodically (image of 4-5 lines) [Fig. 3(a)]. The 13-6 nanowire image showed five dark lines (image of 5 lines) [Fig. 3(b)], and the 14-7-1 image represents images with 5-6 lines [Fig. 3(c)]. The apparent width (the distance between the pair in the image) of the images with 11-4, 12-5, 13-6, and 14-7-1 nanowires appeared to be smaller than the diameter, and are 0.78–0.82 nm (0.85 nm), 0.86–0.89 nm (0.93 nm), 0.98–1.00 nm (1.00 nm) and 1.06–1.08 nm (1.08 nm). These simulated images had the same features as mentioned above regardless of the amount of the degradation. Thus, the platinum nanowire in Fig. 2(a) has a 13-6 multishell structure, although the poor resolution of the platinum image left its period undetermined.

After the platinum nanowire showed the HR-TEM image of Fig. 2(a), the outer layer of the platinum nanowire was partially stripped off by the diffusion of atoms towards the wire end. After the outer shell had been stripped off, the nanowire partially showed a pair of dark lines [Fig. 4(a)]. This pair survived for a few seconds under imaging beam irradiation as intense as 20 A/cm^2 . The apparent widths (the distance between the pair in the TEM image) were kept at 0.4–0.45 nm until the wire snapped. The width was narrower than that of the 7-1 HMS gold nanowire reported so far. The gold 7-1 wire had a diameter of 0.58 nm, and its image had widths of 0.50–0.54 nm.²

We simulated HR-TEM images for 5-0, 6-0, and 7-1 platinum nanowires by multislice calculations to compare with the observed images [Fig. 3(d)–3(f)]. We assumed the same pitch as the inner shell of the 12-5, 13-6, and 14-7-1 gold HMS,² taking $d=0.28$ nm for platinum. The 7-1 model showed an image with 3 lines (image width: 0.52 nm). The 5-0 model showed an image with 2 lines (width: 0.35 nm), whose lines appear to be at asymmetric positions about the wire axis. The 6-0 model (width: 0.40–0.44 nm) also showed an image with 2 lines, whose lines appear to be at symmetric positions about the wire axis and with a width modulation contrast. These image characteristics remain unchanged

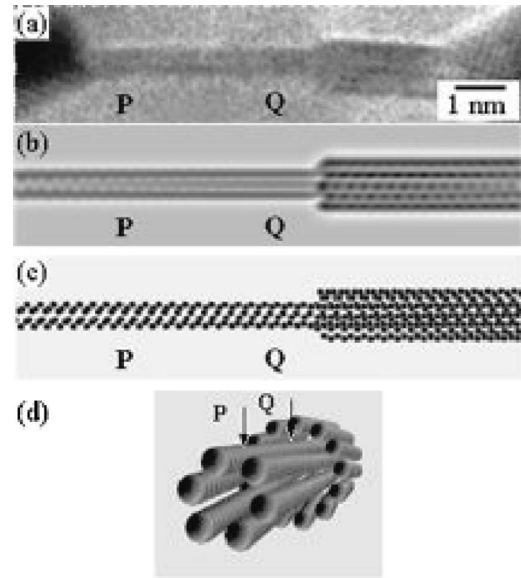


FIG. 4. (a) HR-TEM image of the finest platinum nanotube (left-hand side). This nanowire at the right-hand side is the same as that in Fig. 2(a). The image width is 0.4 nm at position **P**, while it is slightly large at **Q**. (b) Simulated image of a 6-0 nanowire; the outer 13-0 tube was taken off from the 13-6 multishell structure. Two dark lines appear at position **P**, while a faint dark line appears at the wire axis at **Q**. Since the nanotube has a helical structure, the projected image viewed from the incident beam direction is different between positions **P** and **Q** (the incident beam direction is perpendicular to this image). (c) Plane view of an atomic model for the simulation shown in (b). Some of the 6 atomic rows are not resolved with each other for the superposition. (d) Three-dimensional illustration of a 6-membered nanotube joining the 13-6 multishell structure.

qualitatively for different pitches. We further simulated 5-1 and 6-1 models, although they seem to be physically unrealistic; the hollow of the tube is too tight to be filled with an atomic chain. The 5-1 model gives images with 2 asymmetric lines, which have much more uneven contrast than in the 5-0 model. The 6-1 model showed an image with 2 symmetric lines similar to the 6-0 model, but an image of 3 lines appears periodically with an additional central line. In the observed image of Fig. 4(a), two dark lines appear to be symmetric with even contrast. Furthermore, the width of the nanowire increases from the left-hand side (0.4 nm at **P**) to the right-hand side (0.46 nm at **Q**), in accordance with the simulated image for the 6-0 model [Fig. 4(b)].

This modulation of the apparent width of the image is related to the coiling of the platinum atomic row [Fig. 4(c)], since the electron-microscope image is a projection of the 3D structure along the beam direction. The model of the 6-0 nanotube [Fig. 4(c)] explains the above image characteristics. In this image, the apparent width is wider exactly near the point where it goes into a double-wall nanotube. Since the inner and outer nanotubes of gold HMS's have different chirality, and their relative positions are determined uniquely so as to minimize their interfacial energies,¹ we modeled a 13-0 single-wall tube over a 6-0 tube so as to satisfy their relative positions. The image of 13-6 and 6-0 tubes

around the connection is in accord with a simulation without any critical contradiction. The observed platinum nanowire shown in Fig. 4(a) reproduces the width modulation and the appearance of the central faint dark line at around **Q**. Therefore, the finest platinum nanowire in Fig. 4(a) is concluded to be a 6-0 single-wall tube, whose atomic rows coil around the tube axis.

The formation process of the Pt nanowire in Fig. 4(a) suggests that the nanowire on the left-hand side is a single-wall tube which has the same structures as the inner tube at the right-hand side.

The present observation of platinum nanowires gives a certain amount of evidence of a single-wall nanotube having six atomic rows coiling around the axis. When the 13-6

multishell nanowire is stripped off from the outer 13-membered tube, the 6-membered tube becomes exposed. The 6-membered nanotube might be able to stand stationary without the outer tube. In connection with the present analysis, a 5-0 tube is supposed to be formed stably, if electron-beam thinning had started from a 12-5 multishell tube.

In conclusion we found a single-wall platinum nanotube. The nanotube had a diameter of 0.48 nm (the observed widths were 0.40–0.46 nm), and fits with the model structure that six atomic rows coil around the tube axis.

This work was done by the foundation (Quantum Contact: 12002005) from the Ministry of Education of Japan.

*Email address: ohshima@materia.titech.ac.jp

¹Y. Kondo and K. Takayanagi, *Science* **289**, 606 (2001).

²Y. Kondo and K. Takayanagi, *Phys. Rev. Lett.* **79**, 3455 (1997).

³J.M. Krans J.M. van Ruitenbeek, V.V. Fisum, I.K. Yanson, and L.J. de Jongh, *Nature (London)* **375**, 767 (1995).

⁴H. Ohnishi, Y. Kondo, and K. Takayanagi, *Nature (London)* **395**, 780 (1998).

⁵M. Okamoto, T. Uda, and K. Takayanagi, *Phys. Rev. B* **64**, 033303 (2001).

⁶S. Iijima, *Nature (London)* **354**, 56 (1991).

⁷E. Tosatti, S. Prestipino, S. Kostilmeier, A. Dal Corso, and F.D. Di Tolla, *Science* **291**, 288 (2001).

⁸G. Bilalbegović, *Phys. Rev. B* **58**, 15 412 (1998).

⁹G. Bilalbegović *Comp. Mat. Sci.* **18**, 333 (2000).

¹⁰B. Wang, S. Yin, G. Wang, A. Buldum, and J. Zhao, *Phys. Rev. Lett.* **86**, 2046 (2001).

¹¹A.I. Yanson, I.K. Yanson, and J.M. van Ruitenbeek, *Nature (London)* **400**, 144 (1999).

¹²A.I. Yanson, I.K. Yanson, and J.M. van Ruitenbeek, *Phys. Rev. Lett.* **84**, 5832 (2000).

¹³W.A. de Heer, *Rev. Mod. Phys.* **65**, 611 (1993).

¹⁴W.D. Knight, K. Clemenger, W.A. de Heer, W.A. Saunders, M.Y. Chou, and M.L. Cohen, *Phys. Rev. Lett.* **52**, 2141 (1984).

¹⁵I. Katakuse T. Ichihara, Y. Fujita, T. Matsuo, T. Sakurai, and H. Matsuda, *Int. J. Mass Spectrom. Ion Processes* **67**, 229 (1985).

¹⁶I. Katakuse, T. Ichihara, Y. Fujita, T. Matsuo, T. Sakurai, and H. Matsuda, *Int. J. Mass Spectrom. Ion Processes* **69**, 109 (1986).

¹⁷J.L. Costa-Krämer, N. García, and H. Olin, *Phys. Rev. B* **55**, 12 910 (1997).

¹⁸B. Ludoph M.H. Devoret, D. Esteve, C. Urbina, and J.M. van Ruitenbeek, *Phys. Rev. Lett.* **82**, 1530 (1999).

¹⁹K. Hansen, E. Lægsgaard, I. Stensgaard, and F. Besenbacher, *Phys. Rev. B* **56**, 2208 (1997).

²⁰D.W. Pashley, *Adv. Phys.* **5**, 173 (1956).

²¹M.A. Van Hove, R.J. Koestner, P.C. Stair, J.P. Bibérian, L.L. Kesmodel, I. Bartos, and G.A. Somorjai, *Surf. Sci.* **103**, 189 (1981).

²²D. Gibbs, G. Grübel, D.M. Zehner, D.L. Abernathy, and S.G.J. Mochrie, *Phys. Rev. Lett.* **67**, 3117 (1991).

²³J.M. Cowley and A.F. Moodie, *Acta. Cryst.* **10**, 609 (1957).

²⁴M. Mitome and K. Takayanagi, *Ultramicroscopy* **62**, 123 (1996).